JOURNAL OF THEORETICAL
AND APPLIED MECHANICS
50, 1, pp. 23-46, Warsaw 2012
50th anniversary of JTAM

THE INFLUENCE OF MATERIAL PROPERTIES AND CRACK LENGTH ON THE *Q*-STRESS VALUE NEAR THE CRACK TIP FOR ELASTIC-PLASTIC MATERIALS FOR CENTRALLY CRACKED PLATE IN TENSION

Marcin Graba

Kielce University of Technology, Faculty of Mechatronics and Machine Design, Kielce, Poland
e-mail: mgraba@tu.kielce.pl

In the paper, values of the Q-stress determined for various elastic-plastic materials for centre cracked plate in tension (CC(T)) are presented. The influence of the yield strength, the work-hardening exponent and the crack length on the Q-parameter was tested. The numerical results were approximated by closed form formulas. This paper is a continuation of the catalogue of the numerical solutions presented in 2008, which presents Q-stress solutions for single edge notch specimens in bending – SEN(B). Both papers present full numerical results and their approximation for two basic specimens which are used to determine in the laboratory tests the fracture toughness – J-integral, and both specimens are proposed by FITNET procedure used to idealize the real components.

Key words: fracture mechanics, cracks, Q-stress, stress fields, HRR solution, FEM, J-integral, O'Dowd theory

1. Introduction – theoretical backgrounds about *J-Q* theory

The stress field near crack tip for the non-linear Ramberg-Osgood (R-O) material was described in 1968 by Hutchinsonson, who published the fundamental work for fracture mechanics. The presented by Hutchinson solution, now called "the HRR solution", includes the first term of the infinite series only. The numerical analysis shows that the results obtained using the HRR solution are different from the results obtained using the finite element method – FEM (Fig. 1). To eliminate this difference, it is necessary to use more terms in the HRR solution.

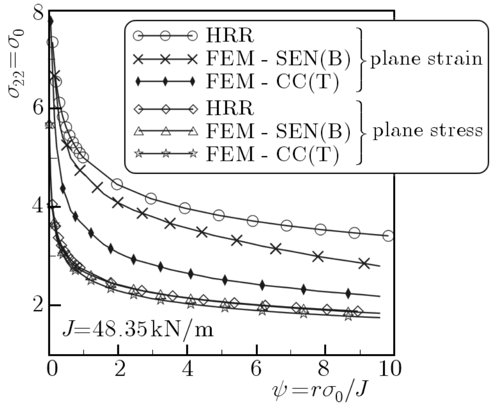

Fig. 1. Comparison of FEM results and HRR solution for the plane stress and plane strain for a single edge notched specimen in bending (SEN(B)) and centrally cracked plate in tension (CC(T)); $E = 206000\,\mathrm{MPa}$, $n = 5$, $\nu = 0.3$, $\sigma_0 = 315\,\mathrm{MPa}$, $\varepsilon_0 = \sigma_0/E = 0.00153$, $a/W = 0.50$, $W = 40\,\mathrm{mm}$, $\theta = 0$

First it was done by Li and Wang (1985), who using two terms in the Airy function, obtained the second term of the asymptotic expansion only for two different materials, described by the R-O exponent equal to $n = 3$ and $n = 10$. Their analysis shows that the two term solution much better describes the stress field near the crack tip, and the value of the second term, which may not to be negligible depends on the material properties and the specimen geometry.

A more accurate solution was proposed by Yang *et al.* (1993), who using the Airy function with the separate variables proposed that the stress field near the crack tip may be described by an infinite series form. The proposed by them solution is currently used with only three terms of the asymptotic solution, and it is often called "J-A_2 theory". Yang *et al.* (1993) conducted full discussion about their idea. They showed that the multi-terms description, which uses three terms of the asymptotic solution is better than the Hutchinson approach. The A_2 amplitude, which is used in the J-A_2 theory suggested by Yang *et al.* (1993) is nearly independent of the distance of the determination, but using the J-A_2 theory in engineering practice is sometimes very burdensome, because an engineer must know the $\widetilde{\sigma}_{ij}^{(k)}$ function and the power exponent t, which are to be calculated by solving a fourth order differential equation, and next using FEM results, the engineer must calculate the A_2 amplitude.

The simplified solution for describing the stress field near the crack tip for elastic plastic materials was proposed by O'Dowd and Shih (1991, 1992). That concept was discussed by Shih *et al.* (1993). They assumed that the FEM results are exact and computed the difference between the numerical and HRR results. They proposed that the stress field near the crack tip may be described by the following equation

$$\sigma_{ij} = \sigma_0\Big(\frac{J}{\alpha\varepsilon_0\sigma_0 I_n(n)r}\Big)^{\frac{1}{n+1}}\widetilde{\sigma}_{ij}(\theta,n) + \sigma_0 Q\Big(\frac{r}{J/\sigma_0}\Big)^q\widehat{\sigma}_{ij}(\theta,n) \tag{1.1}$$

where r and θ are polar coordinates of the coordinate system located at the crack tip, σ_{ij} are the components of the stress tensor, J is the J-integral, n is the R-O exponent, α is the R-O constant, σ_0 – the yield stress, ε_0 – strain related to σ_0 through $\varepsilon_0 = \sigma_0/E$, $\widehat{\sigma}_{ij}(\theta;n)$ are functions evaluated numerically, q is the power exponent whose value changes in the range (0;0.071), and Q is a parameter, which is the amplitude of the second term in the asymptotic solution. The functions $\widetilde{\sigma}_{ij}(n,\theta)$, $I_n(n)$ must be found by solving the fourth order non-linear homogenous differential equation independently for the plane stress and plane strain (Hutchinson, 1968) or these functions may be found using the algorithm and computer code presented in Gałkiewicz and Graba (2006).

O'Dowd and Shih (1991, 1992) tested the Q-parameter in the range $J/\sigma_0 < r < 5J/\sigma_0$ near the crack tip. They showed, that the Q-parameter weakly depends on the crack tip distance in the range of $\pm\pi/2$. They proposed only two terms to describe the stress field near the crack tip

$$\sigma_{ij} = (\sigma_{ij})_{HRR} + Q\sigma_0\widehat{\sigma}_{ij}(\theta) \tag{1.2}$$

where $(\sigma_{ij})_{HRR}$(is the first term of Eq. (1.1) and it is the HRR solution.

To avoid the ambiguity during the calculation of the Q-stress, O'Dowd and Shih (1991, 1992) suggested that the Q-stress should be computed at the distance from the crack tip which is equal to $r = 2J/\sigma_0$ for the direction $\theta = 0$. They postulated that for the $\theta = 0$ direction the function $\widehat{\sigma}_{\theta\theta}(\theta = 0)$ is equal to 1. That is why the Q-stress may be calculated from the following relationship

$$Q = \frac{(\sigma_{\theta\theta})_{FEM} - (\sigma_{\theta\theta})_{HRR}}{\sigma_0} \qquad \text{for } \theta = 0 \quad \text{and} \quad \frac{r\sigma_0}{J} = 2 \tag{1.3}$$

where $(\sigma_{\theta\theta})_{FEM}$ is the stress value calculated using FEM and $(\sigma_{\theta\theta})_{HRR}$ is the stress evaluated form the HRR solution (these are the opening crack tip stress components).

During analysis, O'Dowd and Shih (1991, 1992) showed that the Q-stress value determines the level of the hydrostatic stress. For a plane stress, the Q-parameter is equal to zero or it is close to zero, but for a plane strain, the Q-parameter is in the most cases smaller than zero (Fig. 2). The Q-stress value for a plane strain depends on the external loading and distance from the crack tip – especially for large external loads (Fig. 2b).

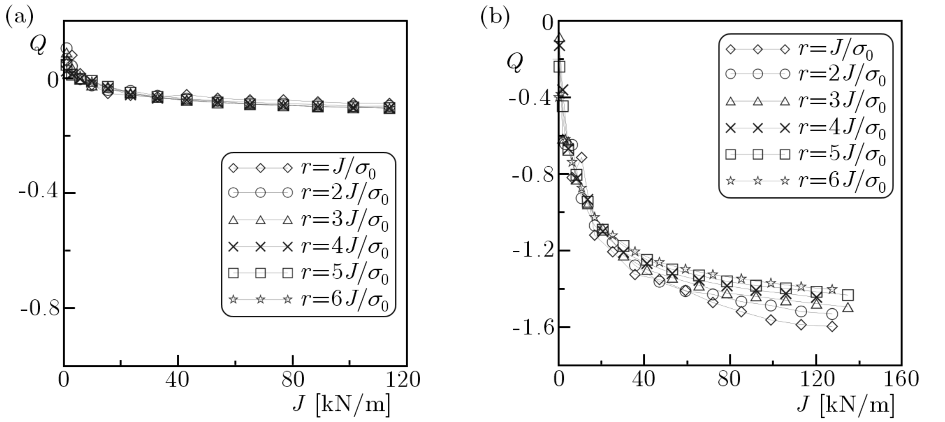

Fig. 2. J-Q trajectories measured at six distances near the crack tip for centrally cracked plate in tension (CC(T)): (a) plane stress, (b) plane strain (own calculation); $W = 40\,\mathrm{mm}$, $a/W = 0.5$, $\sigma_0 = 315\,\mathrm{MPa}$, $\nu = 0.3$, $E = 206000\,\mathrm{MPa}$, $n = 5$

2. Engineering aspects of *J*-*Q* theory, fracture criteria based on the O'Dowd approach

Using the O'Dowd and Shih theory to describe the stress field near the crack tip for elastic-plastic materials, the difference between the HRR solution (Hutchnison, 1968) and the results obtained using the finite element method (FEM) can be eliminated. O'Dowd's theory is quite simple to use in practice, because in order to describe the stress field near the crack tip, we must know only material properties (yield stress, work hardening exponent), J-integral and the Q-stress value, which may be evaluated numerically or determined using the approximation presented in literature, for example Graba (2008). O'Dowd's approach is easier and more convenient to use in contrast to J-A_2 theory, which was proposed by Yang *et al.* (1993). Based on the J-Q theory, O'Dowd (1995) proposed the following fracture criterion

$$J_C = J_{IC}\Big(1 - \frac{Q}{\sigma_c/\sigma_0}\Big)^{n+1} \tag{2.1}$$

where J_C is the real fracture toughness for a structural element characterised by a geometrical constraint defined by Q-stress (whose value is usually is smaller than zero), J_{IC} is the fracture toughness for the plane strain condition for $Q = 0$ and σ_c is the critical stress according to the Ritchie-Knott-Rice hypothesis (Ritchie *et al.*, 1973).

Proposed by O'Dowd fracture criterion was discussed by Neimitz *et al.* (2007), where the authors proposed another form. They modified O'Dowd's formulas (Eq. (2.1)), by replacing the critical stress σ_c by maximum opening stress σ_{max}, which must be evaluated numerically using the large strain formulation. The proposed by Neimitz *et al.* (2007) formulas have the following form

$$J_C = J_{IC}\Big(1 - \frac{Q}{\sigma_{max}/\sigma_0}\Big)^{n+1} \tag{2.2}$$

For a single edge notch in bending (SEN(B)), Neimitz *et al.* (2007) – using the finite element method and the large strain formulation – estimated the maximum opening stress σ_{max} for several materials (different R-O exponents, different yield stresses) and for several crack lengths.

The J-Q theory found application in European Engineering Programs, like SINTAP (1999) or FITNET (2006). The Q-stresses are applied for construction of the fracture criterion and to assess the fracture toughness of structural components. The real fracture toughness K^C_{mat} may be evaluated using the formula proposed by Ainsworth and O'Dowd (1994). They showed that the increase in fracture in both the brittle and ductile regimes may be represented by an expression of the form

$$K^C_{mat} = \begin{cases} K_{mat} & \text{for} \quad \beta L_r > 0 \\ K_{mat}[1 + \alpha(-\beta L_r)^k] & \text{for} \quad \beta L_r < 0 \end{cases} \tag{2.3}$$

where K_{mat} is the fracture toughness for the plane strain condition obtained using FITNET procedures, and β is the parameter calculated using the following formula

$$\beta = \begin{cases} T/(L_r\sigma_0) & \text{for elastic materials} \\ Q/L_r & \text{for elastic-plastic materials} \end{cases} \tag{2.4}$$

where L_r is the ratio of the actual external load P and the limit load P_0 (or the reference stress), which may be calculated using FITNET procedures (FITNET, 2006).

The constants α and k, which are occurring in Eq. (2.3), are material and temperature dependent (Table 1). Sherry *et al.* (2005a,b) proposed procedures to calculate the constants α and k. Thus O'Dowd's theory has practical application to engineering issues.

Sometimes, the J-Q theory may be limited, because there is no value of the Q-stress for a given material and specimen. Using any fracture criterion, for example that proposed by O'Dowd (1995) or another one, Eq. (2.3) (FITNET, 2006) or that presented by Neimitz *et al.* (2007) (see Eq. (2.2)), or presented by Neimitz *et al.* (2004), an engineer can estimate the fracture toughness quite fast, if the Q-stress is known.

Table 1. Some values of the α and k parameters from Eq. (2.3) (SINTAP, 1999; FITNET, 2006)

Material	Temperature	Fracture mode	α	k
A533B (steel)	$-75°C$	cleavage	1.0	1.0
A533B (steel)	$-90°C$	cleavage	1.1	1.0
A533B (steel)	$-45°C$	cleavage	1.3	1.0
Low Carbon Steel	$-50°C$	cleavage	1.3	2.0
A515 (steel)	$+20°C$	cleavage	1.5	1.0
ASTM 710 Grade A	$+20°C$	ductile	0.0	1.0
			0.6	1.0
			1.0	2.0

Literature does not announce the Q-stress catalogue and Q-stress value as functions of the external load, material properties or geometry of the specimen. The numerical analysis shown in Graba (2008) indicates that the Q parameter depends on material properties, specimen geometry and external load. In some papers, an engineer may find J-Q graphs for a certain group of materials. The best solution will be the catalogue of J-Q graphs for materials characterised by various yield strengths, different work-hardening exponents. Such a catalogue should take into consideration the influence of the external load, kind of the specimen (SEN(B) specimen – bending, CC(T) – tension or SEN(T) – tension) and its geometry. For SEN(B) specimens, such a catalogue was presented in Graba (2008), who presented Q-stress values for specimens with predominance of bending for different materials and crack lengths. In the literature, there is no similar catalogue for specimens with predominance of tension. That is why, in the next parts of the paper, values of the Q-stress will be determined for various elastic-plastic materials for a centrally cracked plate in tension (CC(T)). The CC(T) specimen is the basic structural element which is used in the FITNET procedures (FITNET, 2006) to the modelling of real structures. All results will be presented in a graphical form – the $Q = f(J)$ graphs. Next, the numerical results will be approximated by closed form formulas.

3. Details of numerical analysis

In the numerical analysis, the centrally cracked plate in tension (CC(T)) was used (Fig. 3). Dimensions of the specimens satisfy the standard requirement which is set up in FEM calculation $L \geqslant 2W$, where W is the width of the specimen and L is the measuring length of the specimen. Computations were performed for a plane strain using small strain option. The relative crack length was $a/W = \{0.05, 0.20, 0.50, 0.70\}$ where a is the crack length. The width of specimens W was equal to 40 mm (for this case, the measuring length $L \geqslant 80$ mm). All geometrical dimensions of the CC(T) specimen are presented in Table 2.

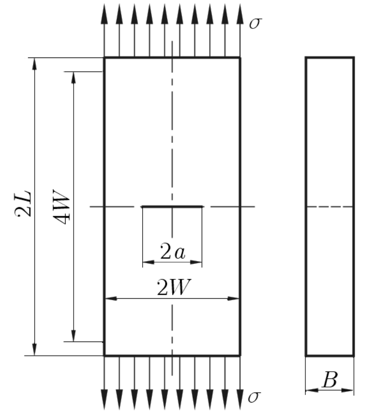

Fig. 3. Centrally cracked plate in tension (CC(T))

Table 2. Geometrical dimensions of the CC(T) specimen used in numerical analysis

width W [mm]	measuring length $4W$ [mm]	total length $2L$ [mm]	relative crack length a/W	crack length a [mm]
40	160	176	0.05	2
			0.20	8
			0.50	20
			0.70	28

The choice of the CC(T) specimen was intentional, because the CC(T) specimens are used in the FITNET procedures (FITNET, 2006) for modelling of real structural elements. Also in the FITNET procedures, the limit load and stress intensity factors for CC(T) specimens are presented. However in the EPRI procedures (Kumar *et al.*, 1981), the hybrid method for calculation of the J-integral, crack opening displacement (COD) or crack tip opening displacement (CTOD) are given. Also some laboratory tests in order to determine the critical values of the J-integral may be done using the CC(T) specimen, see for example Sumpter and Forbes (1992).

Computations were performed using ADINA SYSTEM 8.4 (ADINA, 2006a,b). Due to the symmetry, only a quarter of the specimen was modelled. The finite element mesh was filled with 9-node plane strain elements. The size of the finite elements in the radial direction was decreasing towards the crack tip, while in the angular direction the size of each element was kept constant. The crack tip region was modelled using 36 semicircles. The first of them was 25 times smaller than the last one. It also means that the first finite element behind the crack tip was smaller 2000 times than the width of the specimen. The crack tip was modelled as a quarter of the arc whose radius was equal to $r_w = (1\text{-}2.5) \cdot 10^{-6}$ m. Figure 4 presents exemplary finite element model for CC(T) specimen.

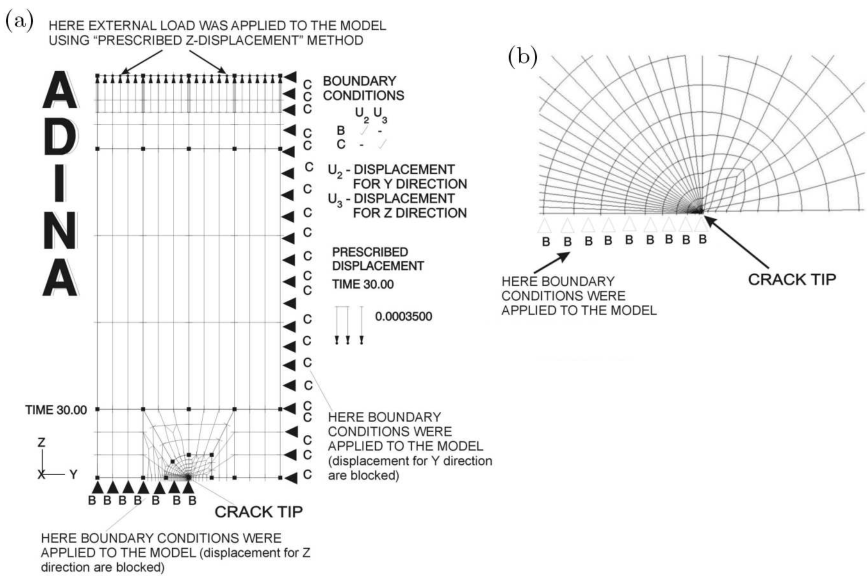

Fig. 4. (a) The finite element model for CC(T) specimen used in the numerical analysis (due to the symmetry, only a quarter of the specimen was modelled); (b) the crack tip model used for the CC(T) specimen

In the FEM simulation, the deformation theory of plasticity and the von Misses yield criterion were adopted. In the model, the stress-strain curve was approximated by the relation

$$\frac{\varepsilon}{\varepsilon_0} = \begin{cases} \sigma/\sigma_0 & \text{for} \quad \sigma \leqslant \sigma_0 \\ \alpha(\sigma/\sigma_0)^n & \text{for} \quad \sigma > \sigma_0 \end{cases} \qquad \text{where} \quad \alpha = 1 \tag{3.1}$$

The tensile properties for materials which were used in the numerical analysis are presented below in Table 3. In the FEM analysis, calculations were done for sixteen materials, which differed by the yield stress and the work hardening exponent.

Table 3. Mechanical properties of the materials used in numerical analysis (σ_0 – yield stress, E – Young's modulusl ν – Poisson's ratio, ε_0 – strain corresponding the yield stress, α – constant in the power law relationship, n work hardening exponent used in Eq. (3.1))

<table>
<tr><th>σ_0 [MPa]</th><th>E [MPa]</th><th>ν</th><th>$\varepsilon_0 = \sigma_0/E$</th><th>$\alpha$</th><th>$n$</th></tr>
<tr><td>315</td><td rowspan="4">206000</td><td rowspan="4">0.3</td><td>0.00153</td><td rowspan="4">1</td><td>3</td></tr>
<tr><td>500</td><td>0.00243</td><td>5</td></tr>
<tr><td>1000</td><td>0.00485</td><td>10</td></tr>
<tr><td>1500</td><td>0.00728</td><td>20</td></tr>
</table>

The J-integral was estimated using the "virtual shift method". It uses the concept of virtual crack growth to compute virtual energy change (ADINA, 2006a,b).

In the numerical analysis, 64 CC(T) specimens were used, which differed by the crack length (different a/W) and material properties (different ratios σ_0/E and values of the power exponent n).

4. Numerical results – analysis of J-Q trajectories for CC(T) specimens

The analysis of the results obtained by the finite element method showed that in the range of distance from the crack tip $J/\sigma_0 < r < 6J/\sigma_0$, the Q-stress decreases if the distance from the crack tip increases (Fig. 5). If the external load increases, the Q-stress decreases and the difference between the Q-stress calculated in the following measurement points (distance r from the crack tip) increases (Fig. 5).

For the sake of the fact that the Q-parameter, which is used in the fracture criterion, is calculated at a distance equal to $r = 2J/\sigma_0$ (which was proposed by O'Dowd and Shih (1991, 1992)), it is necessary to carry out full analysis of the obtained results at this distance from the crack tip.

Assessing the influence of the crack length on the Q-stress value, it is necessary to notice that if the crack length decreases, then the Q-stress reaches a greater negative value for the same J-integral level – see Fig. 6. For CC(T) specimens characterised by a short crack, the J-Q curves reach faster the saturation level than for CC(T) specimens characterised by normative

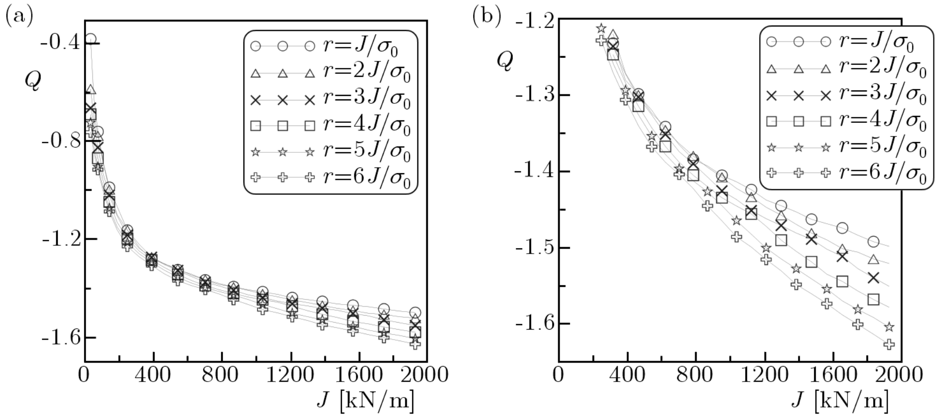

Fig. 5. "The J-Q family curves" for CC(T) specimen calculated at six distances r for plane strain ($W = 40\,\mathrm{mm}$, $a/W = 0.50$, $n = 10$, $\nu = 0.3$, $E = 206000\,\mathrm{MPa}$, $\sigma_0 = 1000\,\mathrm{MPa}$, $\varepsilon_0 = \sigma_0/E = 0.001485$); (a) whole loading spectrum, (b) magnified portion of the graph

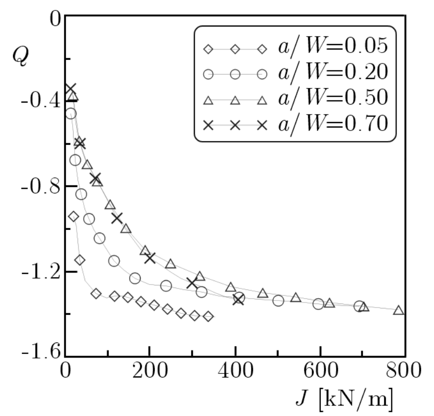

Fig. 6. The influence of the crack length on the J-Q trajectories for CC(T) specimen characterised by $W = 40\,\mathrm{mm}$, $n = 10$, $\nu = 0.3$, $E = 206000\,\mathrm{MPa}$, $\sigma_0 = 1000\,\mathrm{MPa}$, $\varepsilon_0 = \sigma_0/E = 0.00485$ (plane strain at the distance from the crack tip $r = 2J/\sigma_0$)

($a/W = 0.50$) and long ($a/W = 0.70$) cracks. It may be noticed that for short cracks, faster changes of the Q-parameter are observed if the external load increases (see the graphs in Appendices).

As shown in Fig. 7, if the yield stress increases, the Q-parameter increases too, and it reflects for all CC(T) specimens with different crack lengths a/W. For smaller yield stresses, the J-Q trajectories shape up lower, and faster changes of the Q-parameter are observed if the external load is increases

(Fig. 7). Comparing the J-Q trajectories for different values of σ_0/E, it is observed that the biggest differences are characterised for materials with a small work-hardening exponent ($n = 3$ for strongly work-hardening materials) and the smallest for materials characterised by large work-hardening exponents ($n = 20$ for weakly work-hardening materials) – see the graphs in Appendices. If the crack length increases, this difference somewhat increases too. For smaller yield stresses, the J-Q curves for CC(T) specimens reach the saturation level for bigger external loads than the J-Q curves for CC(T) specimens characterised by large yield stresses.

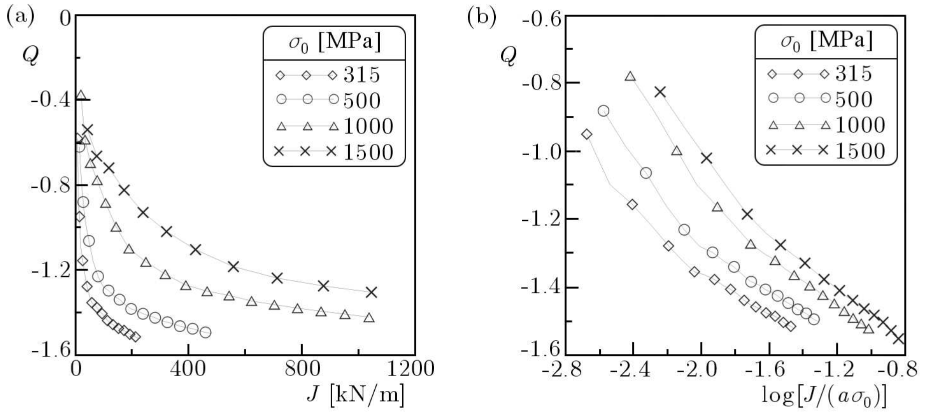

Fig. 7. The influence of the yield stress on J-Q (a) and $Q = f(\log[J/(a\sigma_0)])$ (b) trajectories for CC(T): $W = 40\,\mathrm{mm}$, $a/W = 0.50$, $n = 10$, $\nu = 0.3$, $E = 206000\,\mathrm{MPa}$ (plane strain for the distance from the crack tip $r = 2J/\sigma_0$)

Figures 8 and 9 present some graphs of the J-Q trajectories which show the influence of the work hardening exponent n on the Q-stress value and J-Q curves. If the yield stress decreases, the differences between the J-Q trajectories characterised for materials described by different work-hardening exponents are bigger. For CC(T) specimens, ambiguous behaviour of the J-Q trajectories depending of the work-hardening exponent is observed in comparison with SEN(B) specimens, which was presented in Graba (2008). In most cases (different relative crack lengths a/W, different yield stresses ($\sigma_0/E \geqslant 0.00364$)), if the work-hardening exponent is smaller (strongly work-hardening materials) than the Q-stress value increases (Fig. 9b). For small yield stresses ($0.00153 \leqslant \sigma_/E \leqslant 0.00200$), if the external load increases, then the Q-stress value decreases if the work-hardening exponent decreases (Fig. 8a). For materials characterised by the yield stress $\sigma_0/E = 0.00243$, the difference between the J-Q trajectories are small. Mutual intersecting and overlapping of the trajectories are observed too (Fig. 9a).

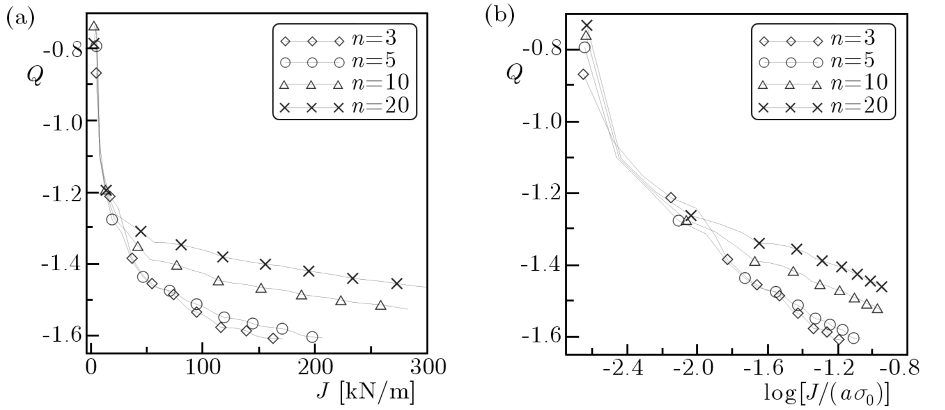

Fig. 8. The influence of the work-hardening exponent on J-Q (a) and $Q = f(\log[J/(a\sigma_0)])$ (b) trajectories for CC(T): $W = 40\,\mathrm{mm}$, $a/W = 0.20$, $\nu = 0.3$, $E = 206000\,\mathrm{MPa}$, $\sigma_0 = 315\,\mathrm{MPa}$, $\varepsilon_0 = \sigma_0/E = 0.00153$ (plane strain for the distance from the crack tip $r = 2J/\sigma_0$)

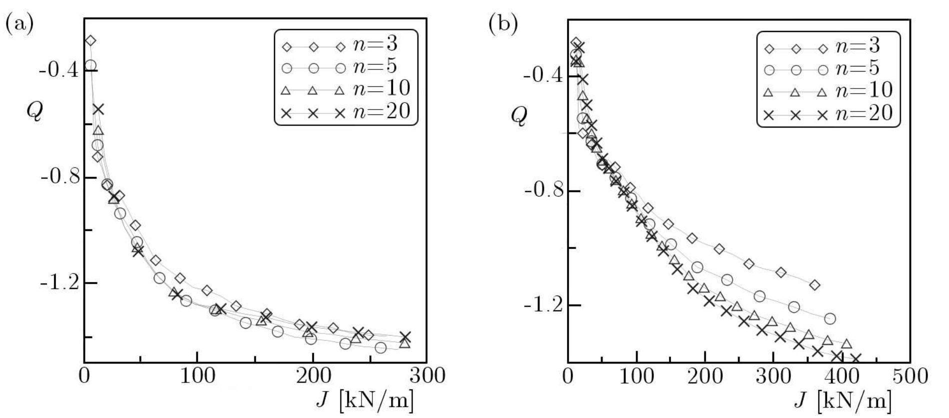

Fig. 9. The influence of the work-hardening exponent on J-Q trajectories for CC(T): $W = 40\,\mathrm{mm}$, $\nu = 0.3$, $E = 206000\,\mathrm{MPa}$ and (a) $a/W = 0.50$, $\sigma_0 = 500\,\mathrm{MPa}$, $\varepsilon_0 = \sigma_0/E = 0.00243$, (b) $a/W = 0.70$, $\sigma_0 = 1000\,\mathrm{MPa}$, $\varepsilon_0 = \sigma_0/E = 0.00485$ (plane strain for the distance from the crack tip $r = 2J/\sigma_0$)

5. Approximation of the numerical results for CC(T) specimens

All the obtained in the numerical analysis results were used to create a catalogue of the J-Q trajectories for different specimens (characterised by different loading application, crack length) and different materials. The presented in the paper results are complementary with the directory presented in 2008 for SEN(B) specimens (Graba, 2008). The current paper gives full numerical results for specimens with predominance of tension. The previous paper, which was mentioned above, gave numerical results and their approximation for specimens with predominance of bending.

The presented numerical computations provided the J-Q catalogue and universal formula (5.1) which allows one to calculate the Q-stress for CC(T) specimens and take into consideration all the parameters influencing the value of the Q-stress. All results were presented in the $Q = f(\log[J/(a\sigma_0)])$ graph forms (for example see Fig. 8b and Fig. 10).

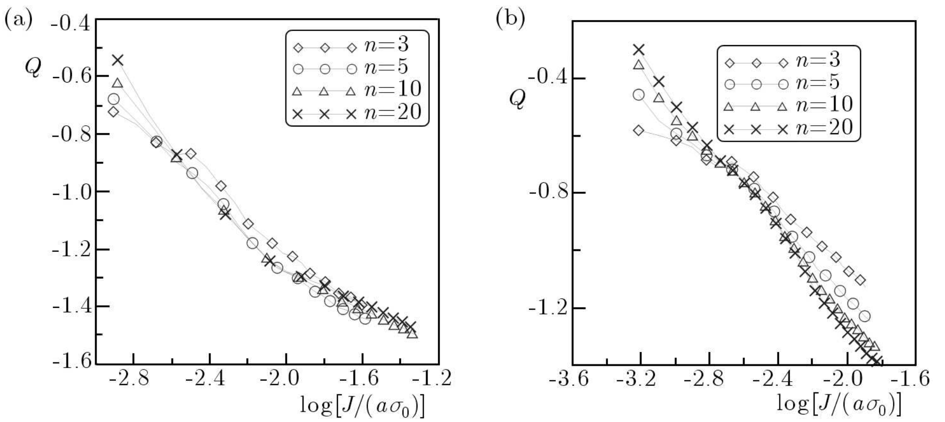

Fig. 10. The influence of the work-hardening exponent on $Q = f(\log[J/(a\sigma_0)])$ trajectories for SEN(B) specimen: $W = 40\,\mathrm{mm}$, $\nu = 0.3$, $E = 206000\,\mathrm{MPa}$, (a) $a/W = 0.50$, $\sigma_0 = 500\,\mathrm{MPa}$, $\varepsilon_0 = \sigma_0/E = 0.00243$ and (b) $a/W = 0.70$, $\sigma_0 = 1000\,\mathrm{MPa}$, $\varepsilon_0 = \sigma_0/E = 0.00485$; which were used in the procedure of approximation

Next, all graphs were approximated by simple mathematical formulas taking the material properties, external load and geometry of the specimen into consideration. All the approximations were made for the results obtained at the distance $r = 2J/\sigma_0$. Each of the obtained trajectories $Q = f(\log[J/(a\sigma_0)])$ was approximated by the third order polynomial in the form

$$Q(J, a, \sigma_0) = A + B \log \frac{J}{a\sigma_0} + C\Big(\log \frac{J}{a\sigma_0}\Big)^2 + D\Big(\log \frac{J}{a\sigma_0}\Big)^3 \tag{5.1}$$

where the A, B, C, D coefficients depend on the work-hardening exponent n, yield stress σ_0 and crack length a/W. The rank of the fitting of formula (5.1) to numerical results for the worst case was equal $R^2 = 0.94$ for the crack length $a/W = 0.05$. For other crack lengths $a/W = \{0.20, 0.50, 0.70\}$, the rank of the fitting of formula (5.1) satisfied the condition $R^2 \geqslant 0.99$. For different work hardening exponents n, yield stresses σ_0 and ratios a/W, which were not included in the numerical analysis, the coefficients A, B, C and D may be evaluated using the linear or quadratic approximation. The results of numerical approximation using formula (5.1) for CC(T) specimens (all coefficients and the rank of the fitting) are presented in Tables 4-7.

Table 4. Coefficients of equation (5.1) for CC(T) specimen with the crack length $a/W = 0.05$

n	A	B	C	D	R^2
$\sigma_0 = 315\,\mathrm{MPa},\ \sigma_0/E = 0.00153$					
3	−1.79540	−0.16046	0.00270	−0.05173	0.979
5	−1.84658	−0.29915	−0.12998	−0.07354	0.982
10	−1.84196	−0.61308	−0.41668	−0.13219	0.961
20	−1.74217	−0.60418	−0.44835	−0.13965	0.939
$\sigma_0 = 1000\,\mathrm{MPa},\ \sigma_0/E = 0.00485$					
3	−1.54832	−0.56730	−0.33063	−0.11413	0.982
5	−1.72656	−0.63071	−0.33882	−0.10721	0.986
10	−1.49156	−0.10931	−0.03536	−0.05032	0.989
20	−1.60795	−0.40632	−0.28062	−0.10566	0.996
$\sigma_0 = 500\,\mathrm{MPa},\ \sigma_0/E = 0.00243$					
3	−1.61802	−0.35121	−0.26183	−0.12290	0.991
5	−1.74621	−0.47823	−0.33828	−0.12560	0.980
10	−1.79245	−0.70894	−0.52808	−0.16144	0.969
20	−1.74847	−0.77333	−0.63058	−0.18304	0.934
$\sigma_0 = 1500\,\mathrm{MPa},\ \sigma_0/E = 0.00728$					
3	−1.33418	−0.24308	−0.05234	−0.04542	0.951
5	−1.51558	−0.28024	−0.05331	−0.03969	0.970
10	−1.52391	−0.19560	−0.02477	−0.03644	0.981
20	−1.59474	−0.30780	−0.10917	−0.05471	0.984

Table 5. Coefficients of equation (5.1) for CC(T) specimen with the crack length $a/W = 0.20$

n	A	B	C	D	R^2
$\sigma_0 = 315\,\mathrm{MPa},\ \sigma_0/E = 0.00153$					
3	−3.40016	−2.97172	−1.63678	−0.33292	0.995
5	−2.81279	−2.11444	−1.22345	−0.26738	0.990
10	−2.23934	−1.40529	−0.89907	−0.21962	0.999
20	−2.13638	−1.32808	−0.84394	−0.20595	1.000

$\sigma_0 = 1000\,\mathrm{MPa},\ \sigma_0/E = 0.00485$					
3	−3.65130	−3.39214	−1.55538	−0.26722	0.973
5	−1.67933	−0.35103	−0.11710	−0.05261	0.995
10	−1.49619	−0.12541	−0.07218	−0.05963	0.997
20	−1.53751	−0.18282	−0.11915	−0.07285	0.991
$\sigma_0 = 500\,\mathrm{MPa},\ \sigma_0/E = 0.00243$					
3	−2.27413	−1.18967	−0.58590	−0.13421	0.992
5	−2.29981	−1.38659	−0.81232	−0.19438	0.997
10	−2.42665	−1.88288	−1.19659	−0.27781	0.998
20	−2.57462	−2.29845	−1.48745	−0.33839	0.997
$\sigma_0 = 1500\,\mathrm{MPa},\ \sigma_0/E = 0.00728$					
3	−1.27982	0.01996	0.14503	0.01481	0.989
5	−1.41550	−0.01120	0.11191	−0.00153	0.994
10	−1.54844	−0.25319	−0.11256	−0.06390	0.993
20	−1.67907	−0.45441	−0.25880	−0.10071	0.994

Table 6. Coefficients of equation (5.1) for CC(T) specimen with the crack length $a/W = 0.50$

n	A	B	C	D	R^2
$\sigma_0 = 315\,\mathrm{MPa},\ \sigma_0/E = 0.00153$					
3	−3.85021	−2.64950	−1.05024	−0.17336	0.990
5	−2.54684	−1.13625	−0.51015	−0.11358	0.997
10	−2.24656	−0.98456	−0.50146	−0.11605	0.997
20	−3.18413	−2.55066	−1.29798	−0.24468	0.996
$\sigma_0 = 1000\,\mathrm{MPa},\ \sigma_0/E = 0.00485$					
3	−3.42176	−2.52110	−0.90895	−0.13071	0.977
5	−1.63674	0.01781	0.19411	0.01940	0.994
10	−1.68070	−0.08345	0.05407	−0.02520	0.997
20	−1.88835	−0.39917	−0.13029	−0.06196	0.996
$\sigma_0 = 500\,\mathrm{MPa},\ \sigma_0/E = 0.00243$					
3	−3.55938	−2.47891	−0.95900	−0.15488	0.983
5	−0.96124	1.06111	0.56236	0.05471	0.998
10	−1.61943	−0.06732	−0.04079	−0.04818	0.999
20	−2.39669	−1.42289	−0.78360	−0.17829	0.999

$\sigma_0 = 1500\,\mathrm{MPa},\ \sigma_0/E = 0.00728$					
3	−1.27394	−0.01699	0.04887	−0.01944	0.997
5	−1.57516	−0.02788	0.20193	0.03045	0.994
10	−1.94130	−0.43244	0.01182	−0.00341	0.994
20	−2.07357	−0.56398	−0.06157	−0.02087	0.995

Table 7. Coefficients of equation (5.1) for CC(T) specimen with the crack length $a/W = 0.70$

n	A	B	C	D	R^2
$\sigma_0 = 315\,\mathrm{MPa},\ \sigma_0/E = 0.00153$					
3	−3.39313	−1.86453	−0.70116	−0.12257	0.991
5	−1.86720	−0.11810	−0.07379	−0.05049	0.998
10	−3.70437	−2.86445	−1.35357	−0.24114	0.997
20	−5.11211	−4.87495	−2.27736	−0.37934	0.997
$\sigma_0 = 1000\,\mathrm{MPa},\ \sigma_0/E = 0.00485$					
3	−2.93370	−1.54934	−0.40487	−0.04995	0.986
5	−2.16067	−0.26326	0.17639	0.02853	0.997
10	−2.42945	−0.26930	0.25072	0.04251	0.998
20	−2.39733	−0.11232	0.32626	0.05005	0.998
$\sigma_0 = 500\,\mathrm{MPa},\ \sigma_0/E = 0.00243$					
3	−6.77352	−5.84374	−2.12683	−0.28448	0.981
5	−2.14513	−0.20561	0.07296	−0.00700	0.997
10	−2.09694	−0.47913	−0.18855	−0.06352	0.998
20	−2.21086	−0.88306	−0.48750	−0.12529	0.999
$\sigma_0 = 1500\,\mathrm{MPa},\ \sigma_0/E = 0.00728$					
3	−2.02517	−0.78494	−0.17842	−0.02840	0.992
5	−2.05092	−0.46715	0.02955	0.00524	0.989
10	−2.10385	−0.19800	0.21559	0.03379	0.992
20	−2.31937	−0.32264	0.19251	0.03093	0.996

Figure 11 presents the comparison of the numerical results and their approximation for J-Q trajectories for several cases of the CC(T) specimens. Appendices A-D attached to the paper present in a graphical form (Figs. 12-15) all numerical results obtained for CC(T) specimens in plain strain. All results are presented using the J-Q trajectories for each analyzed case.

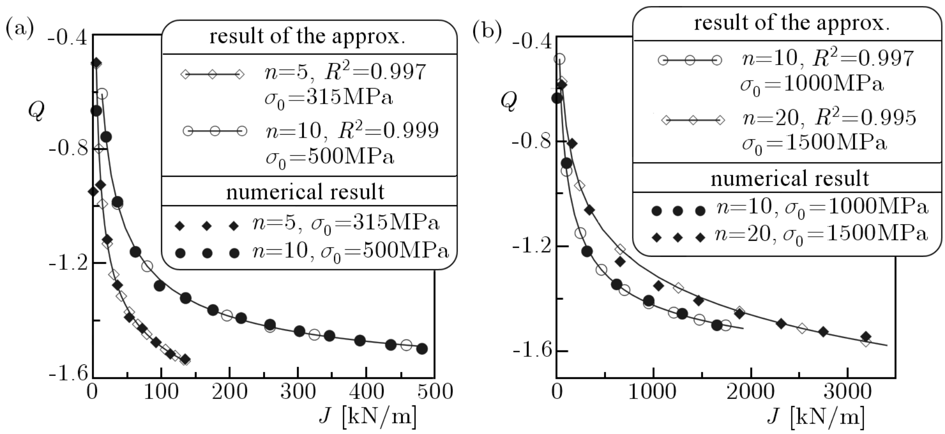

Fig. 11. Comparison of the numerical results and their approximation for J-Q trajectories for CC(T) specimens: $W = 40\,\mathrm{mm}$, $a/W = 0.50$, $E = 206000\,\mathrm{MPa}$, $\nu = 0.3$ and (a) $\sigma_0 \in \{315, 500\}\,\mathrm{MPa}$, $n \in \{5, 10\}$, (b) $\sigma_0 \in \{1000, 1500\}\,\mathrm{MPa}$, $n \in \{10, 20\}$

6. Conclusions

In the paper, values of the Q-stress were determined for various elastic-plastic materials for centrally cracked plate in tension (CC(T)). The influence of the yield strength, the work-hardening exponent and the crack length on the Q-parameter was tested. The numerical results were approximated by closed form formulas. In summary, it may be concluded that the Q-stress depends on geometry and the external load. Different values of the Q-stress are obtained for a centrally cracked plane in tension (CC(T)) and different for the SEN(B) specimen, which was characterised by the same material properties (see Appendices of this paper and Appendices in Graba (2008)). The Q-parameter is a function of the material properties; its value depends on the work-hardening exponent n and the yield stress σ_0. If the crack length decreases, then Q-stress reaches greater negative value for the same external load.

The presented in the paper catalogue of the Q-stress values and J-Q trajectories for specimens with predominance of tension (CC(T) specimens) is complementary with the numerical solution presented in Graba (2008), which gave J-Q trajectories for specimens with predominance of bending (SEN(B) specimens)). Both papers may be quite useful for solving engineering problems in which the fracture toughness or stress distribution near the crack tip must be quite fast estimated.

Appendix A. Numerical results for CC(T) specimen in plane strain with the crack length $a/W = 0.05$ (distance from the crack tip $r = 2J/\sigma_0$)

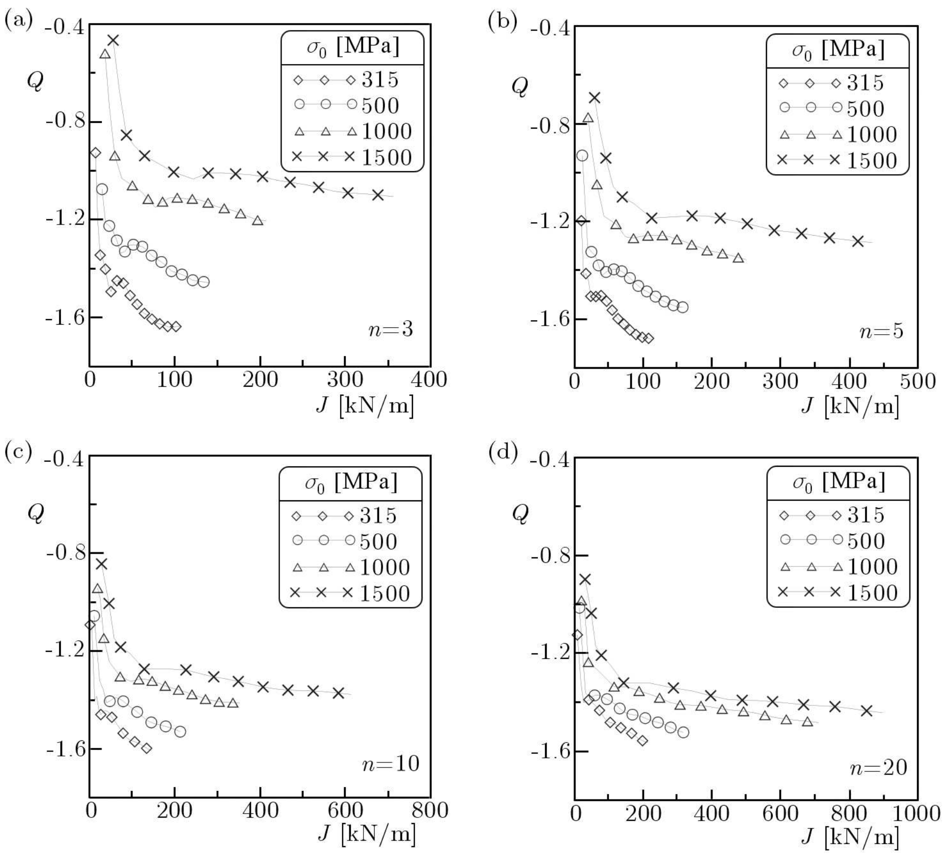

Fig. 12. The influence of the yield stress on J-Q trajectories for CC(T) specimens with the crack length $a/W = 0.05$ for different power exponents in R-O relationship: (a) $n = 3$, (b) $n = 5$, (c) $n = 10$, (d) $n = 20$ ($W = 40\,\mathrm{mm}$, $\nu = 0.3$, $E = 206000\,\mathrm{MPa}$)

Appendix B. Numerical results for CC(T) specimen in plane strain with the crack length $a/W = 0.20$ (distance from the crack tip $r = 2J/\sigma_0$)

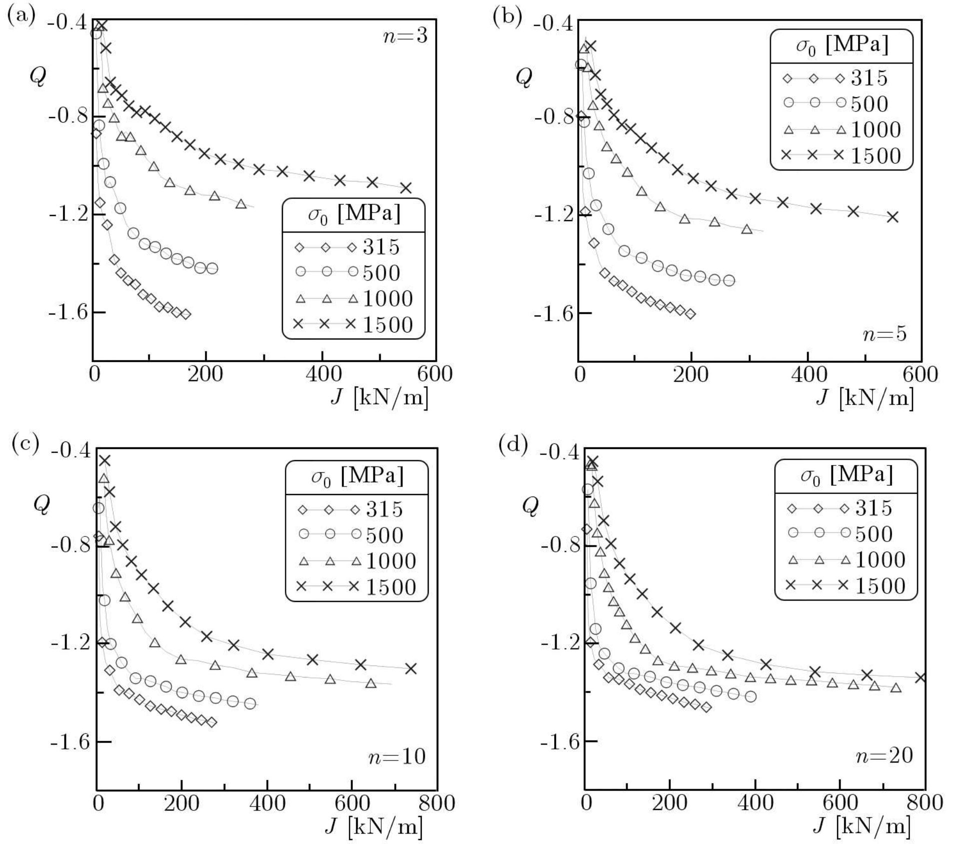

Fig. 13. The influence of the yield stress on J-Q trajectories for CC(T) specimens with the crack length $a/W = 0.20$ for different power exponents in R-O relationship: (a) $n = 3$, (b) $n = 5$, (c) $n = 10$, (d) $n = 20$ ($W = 40\,\mathrm{mm}$, $\nu = 0.3$, $E = 206000\,\mathrm{MPa}$)

Appendix C. Numerical results for CC(T) specimen in plane strain with the crack length $a/W = 0.50$ (distance from the crack tip $r = 2.J/\sigma_0$)

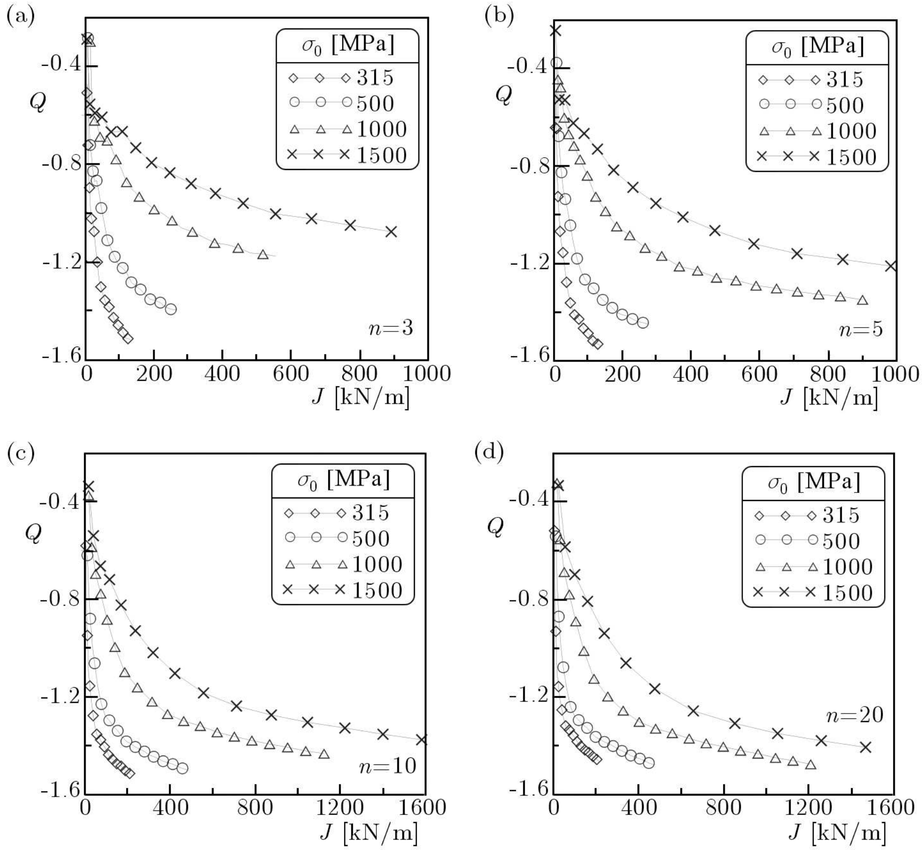

Fig. 14. The influence of the yield stress on J-Q trajectories for CC(T) specimens with the crack length $a/W = 0.50$ for different power exponents in R-O relationship: (a) $n = 3$, (b) $n = 5$, (c) $n = 10$, (d) $n = 20$ ($W = 40\,\mathrm{mm}$, $\nu = 0.3$, $E = 206000\,\mathrm{MPa}$)

Appendix D. Numerical results for CC(T) specimen in plane strain with the crack length $a/W = 0.70$ (distance from the crack tip $r = 2J/\sigma_0$)

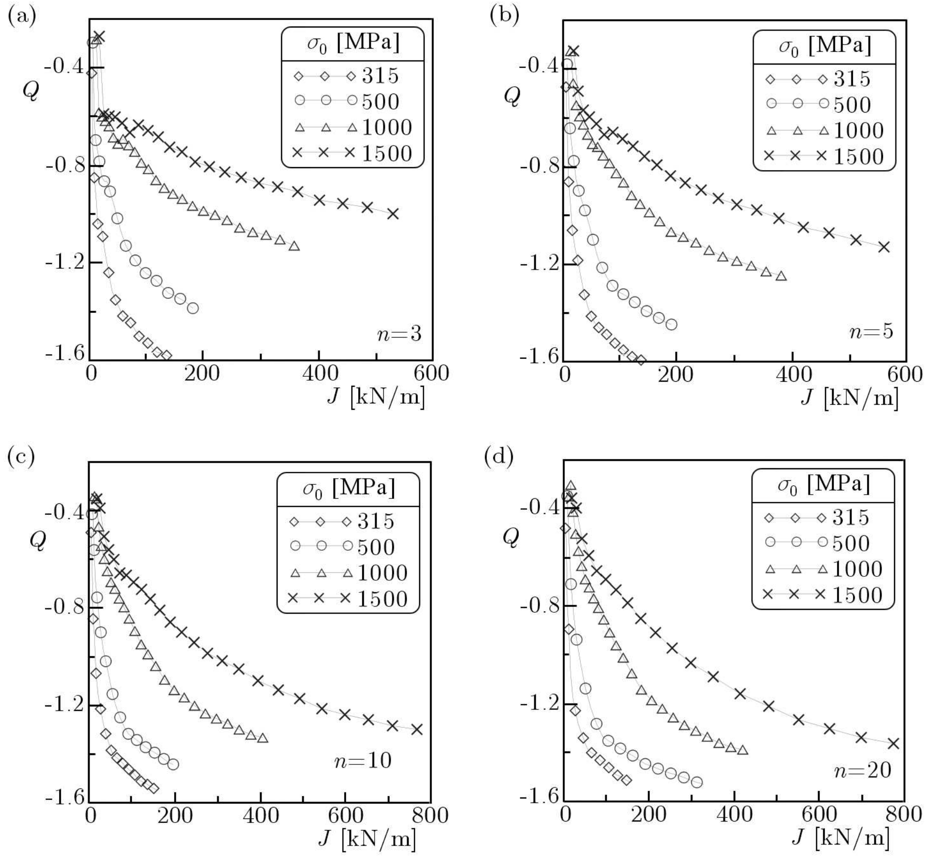

Fig. 15. The influence of the yield stress on J-Q trajectories for CC(T) specimens with the crack length $a/W = 0.70$ for different power exponents in R-O relationship: (a) $n = 3$, (b) $n = 5$, (c) $n = 10$, (d) $n = 20$ ($W = 40\,\text{mm}$, $\nu = 0.3$, $E = 206000\,\text{MPa}$)

Acknowledgements

The support of Kielce University of Technology, Faculty of Mechatronics and Machine Design through grant No. 1.22/8.57 is acknowledged by the author of the paper.

References

1. ADINA 2006a, ADINA 8.4.1: User Interface Command Reference Manual – Volume I: ADINA Solids & Structures Model Definition, Report ARD 06-2, ADINA R&D, Inc.
2. ADINA 2006b, ADINA 8.4.1: Theory and Modeling Guide – Volume I: ADINA, Report ARD 06-7, ADINA R&D, Inc.
3. Ainsworth R.A., O'Dowd N.P., 1994, A framework of including constraint effects in the failure assessment diagram approach for fracture assessment, *ASME Pressure Vessels and Piping Conference*, *ASME*, PVP-Vol 287/MD-Vol 47
4. FITNET, 2006, FITNET Report, (European Fitness-for-service Network), Edited by M. Kocak, S. Webster, J.J. Janosch, R.A. Ainsworth, R. Koers, Contract No. G1RT-CT-2001-05071
5. Gałkiewicz J., Graba M., 2006, Algorithm for determination of $\widetilde{\sigma}_{ij}(n,\theta)$, $\widetilde{\varepsilon}_{ij}(n,\theta)$, $\widetilde{u}_i(n,\theta)$, $d_n(n)$, and $I_n(n)$ functions in Hutchinson-Rice-Rosengren solution and its 3D generalization, *Journal of Theoretical and Applied Mechanics*, **44**, 1, 19-30
6. Graba M., 2008, The influence of material properties on the Q-stress value near the crack tip for elastic-plastic materials, *Journal of Theoretical and Applied Mechanics*, **46**, 2, 269-290
7. Hutchinson J.W., 1968, Singular behaviour at the end of a tensile crack in a hardening material, *Journal of the Mechanics and Physics of Solids*, **16**, 13-31
8. Kumar V., German M.D., Shih C.F., 1981, An engineering approach for elastic-plastic fracture analysis, *EPRI Report NP-1931*, Electric Power Research Institute, Palo Alto, CA
9. Li Y., Wang Z., 1985, High-order asymptotic field of tensile plane-strain nonlinear crack problems, *Scientia Sinica (Series A)*, **XXIX**, 9, 941-955
10. Neimitz A., Dzioba I., Molasy R., Graba M., 2004, Wpływ więzów na odporność na pękanie materiałów kruchych, *Materiały XX Sympozjum Zmęczenia i Mechaniki Pękania*, Bydgoszcz-Pieczyska, 265-272
11. Neimitz A., Graba M., Gałkiewicz J., 2007, An alternative formulation of the Ritchie-Knott-Rice local fracture criterion, *Engineering Fracture Mechanics*, **74**, 1308-1322
12. O'Dowd N.P., 1995, Applications of two parameter approaches in elastic-plastic fracture mechanics, *Engineering Fracture Mechanics*, **52**, 3, 445-465
13. O'Dowd N.P., Shih C.F., 1991, Family of crack-tip fields characterized by a triaxiality parameter – I. Structure of fields, *J. Mech. Phys. Solids*, **39**, 8, 989-1015

14. O'DOWD N.P., SHIH C.F., 1992, Family of crack-tip fields characterized by a triaxiality parameter – II. Fracture applications, *J. Mech. Phys. Solids*, **40**, 5, 939-963

15. RITCHIE R.O., KNOTT J.F., RICE J.R., 1973, On the relationship between critical tensile stress and fracture toughness in mild steel, *Journal of the Mechanics and Physics of Solids*, **21**, 395-410

16. SINTAP, 1999, SINTAP: Structural Integrity Assessment Procedures for European Industry. Final Procedure, Brite-Euram Project No. BE95-1426 – Rotherham: British Steel

17. SHERRY, A.H., WILKES M.A., BEARDSMORE D.W., LIDBURY D.P.G., 2005a, Material constraint parameters for the assessment of shallow defects in structural componenets – Part I: Parameter solutions, *Engineering Fracture Mechanics*, **72**, 2373-2395

18. SHERRY A.H., HOOTON D.G., BEARDSMORE D.W., LIDBURY D.P.G., 2005b, Material constraint parameters for the assessment of shallow defects in structural components – Part II: Constraint – based assessment of shallow cracks, *Engineering Fracture Mechanics*, **72**, 2396-2415

19. SHIH C.F., O'DOWD N.P., KIRK M.T., 1993, A framework for quantifying crack tip constraint, [In:] *Constraint Effects in Fracture*, ASTM STP 1171, E.M. Hackett, K,-H. Schwalbe, R.H. Dodds, Eds., American Society for Testing and Materials, Philadelphia, 2-20

20. SUMPTER J.D.G., FORBES A.T., 1992, Constraint based analysis of shallow cracks in mild steel, *TWI/EWI/IS International Conference on Shallow Crack Fracture Mechanics Test and Application*, M.G. Dawes, Edit., Cambridge, UK, paper 7

21. YANG S., CHAO Y.J., SUTTON M.A., 1993, Higher order asymptotic crack tip in a power-law hardening material, *Engineering Fracture Mechanics*, **45**, 1, 99-120

Wpływ stałych materiałowych i długości pęknięcia na rozkład naprężeń Q przed wierzchołkiem pęknięcia w materiałach sprężysto-plastycznych dla płyty z centralną szczeliną poddanej rozciąganiu

Streszczenie

W pracy przedstawione zostały wartości naprężeń Q wyznaczone dla szeregu materiałów sprężysto-plastycznych dla płyt z centralną szczeliną na wskroś poddawanych rozciąganiu (CC(T)). Omówiony został wpływ granicy plastyczności i wykładnika umocnienia na wartość naprężeń Q, a także wpływ długości pęknięcia. Wyniki

obliczeń numerycznych aproksymowano formułami analitycznymi. Rezultaty pracy stanowią podręczny katalog krzywych J-Q dla próbek CC(T) – próbek z przewagą rozciągania, możliwy do wykorzystania w praktyce inżynierskiej. Prezentowane wyniki są kontynuacją katalogu zaprezentowanego w roku 2008], który zawierał numeryczne rozwiązania i ich aproksymacje dla próbek z przewagą zginania (próbki SEN(B)). Oba elementy konstrukcyjne (próbki CC(T) i SEN(B)) często są wykorzystywane do wyznaczania odporności na pękanie w warunkach laboratoryjnych, a w analizie inżynierskiej stosuje się je jako uproszczenie złożonego obiektu konstrukcyjnego, co zalecane jest w procedurach FITNET.

Manuscript received August 13, 2010; accepted for print April 4, 2011